https://doi.org/10.5194/egusphere-2024-2785
Preprint. Discussion started: 24 September 2024

Disentangling Atmospheric, Hydrological, and Coupling Uncertainties in Compound Flood Modeling within a Coupled Earth System Model

Dongyu Feng[1], Zeli Tan[1], Darren Engwirda[2], Jonathan D. Wolfe[2], Donghui Xu[1], Chang Liao[1], Gautam Bisht[1], James J. Benedict[2], Tian Zhou[1], Mithun Deb[3], Hong-Yi Li[4], and L. Ruby Leung[1]

[1]Atmospheric, Climate, & Earth Sciences Division, Pacific Northwest National Laboratory, Richland, WA, 99354, USA
[2]T-3 Fluid Dynamics and Solid Mechanics Group, Los Alamos National Laboratory, Los Alamos, NM, 87545, USA
[3]Marine and Coastal Research Laboratory, Pacific Northwest National Laboratory, Sequim, WA, 98382, USA
[4]Department of Civil and Environmental Engineering, University of Houston, TX, 77204, USA

Correspondence to: Dongyu Feng (dongyu.feng@pnnl.gov)

Abstract. Compound riverine and coastal flooding is usually driven by complex interactions among meteorological, hydrological, and ocean extremes. However, existing efforts of modeling this phenomenon often rely on models that do not integrate hydrological processes across atmosphere-land-river-ocean systems, leading to substantial uncertainties that have not been fully examined. To bridge the gap, we leverage the new capabilities of the Energy Exascale Earth System Model (E3SM) that enable a multi-component framework that integrates coastal-refined atmospheric, terrestrial, and oceanic components. We evaluate compound uncertainties arising from two-way land-river-ocean coupling in E3SM, and track the cascading meteorological and hydrological uncertainties through ensemble simulations over the Delaware River basin and estuary during Hurricane Irene (2011). Our findings highlight the importance of two-way river-ocean coupling to compound flood modeling and demonstrate E3SM's effectiveness in handling multivariate flooding on the coast. Our study shows the growing uncertainties that transition from atmospheric forcings to flood distribution and severity. Furthermore, an Artificial Neural Network based analysis is used to assess the roles of some understudied hydrological drivers, such as infiltration and soil moisture, in the generation of compound flooding. The response of compound floods to tropical cyclones (TCs) is found to be susceptible to these often overlooked drivers. For instance, flood damage could be tripled if Hurricane Irene was preceded by an extreme antecedent soil moisture condition (AMC). The results not only support the use of a multi-component framework for interactive flooding processes, but also underscore the necessity of broader definitions of compound flooding that encompasses the simultaneous occurrence of intense precipitation, storm surge, and high AMC during TCs.

Keywords: Earth System Model, hydrologic modeling, compound flooding, antecedent soil moisture condition

https://doi.org/10.5194/egusphere-2024-2785
Preprint. Discussion started: 24 September 2024

1 Introduction

Compound flooding (CF) is a significant and complex hazard encompassing multiple concurrent drivers such as heavy rainfall, storm surges, and rain-on-snow events (Li et al., 2019) that cause severe socioeconomic and environmental damages (Zscheischler et al., 2018). In coastal regions, CF often arises from a complex interplay of meteorological, hydrological, fluvial, and oceanic processes triggered by tropical cyclones (TCs) (Leonard et al., 2014; Bilskie and Hagen, 2018; Hendry et al., 2019; Loveland et al., 2021). Characterized by high wind speeds and low surface atmospheric pressure, TCs can bring intense rainfall over land and significant storm surge above normal tide levels (Fig. 1). CF poses elevated risks compared to single-source pluvial, fluvial, and coastal flooding due to its broader spatial coverage and extended durations (Wahl et al., 2015; Moftakhari et al., 2017). Sarhadi et al. (2024) suggested that the frequency and intensity of CF events would increase by up to fivefold by the end of this century, driven by factors such as intensified TCs and rising sea levels (Feng et al., 2022). This bleak projection highlights the critical need for advanced integrated modeling strategies, aiming to effectively mitigate future flood risks and improve the resilient infrastructure and adaptive community response plans (Bates et al., 2021).

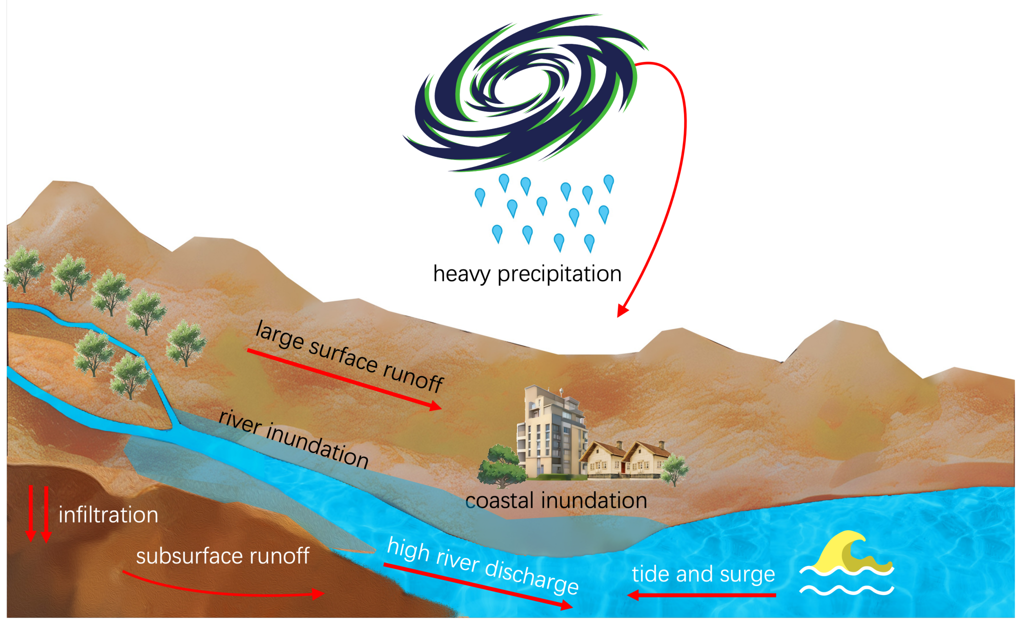

Figure 1: Compound flooding processes in a coastal river basin during a TC event. This conceptual diagram shows the key elements contributing to CF, resulting from combined riverine and coastal inundation along the river channels and adjacent coastal areas.

Modeling CF is inherently challenging because CF is triggered and governed by the interactions of processes in multiple earth system components, including atmosphere, land, river, and ocean (Xu et al., 2023). Traditional modeling approaches that rely on one-way coupling between any two model components thus have a limited ability to capture CF (Santiago-Collazo et al., 2019). The Energy Exascale Earth System Model (E3SM) represents a significant advancement in Earth System modeling (Golaz et al., 2019, 2022). As a state-of-the-science model, E3SM features a tightly integrated multi-component framework that supports dynamic exchanges and propagation of information across its different components, such as two-way land-river coupling (Xu et al., 2022b) and two-way river-ocean coupling (Feng et al., 2022). Additionally, several other developments were recently implemented that further improve the modeling of coastal CF, including the introduction of high-resolution coastal-refined meshes (Feng et al., 2022), the implementation of interactively coupled land-river-ocean models (Xu et al., 2022b; Feng et al., 2024), and variable-resolution ocean time-stepping (Lilly et al., 2023). Compared with regional models that may provide more detailed inundation at the street level (Costabile et al., 2023; Ivanov et al., 2021), E3SM excels at coupling processes across various earth system components. This capability is crucial for capturing the complex responses of earth systems to climate change and projecting climate-driven flood hazards.

While a coupled model is needed to study CF, this advancement can inevitably introduce additional uncertainties. For instance, compared with atmospheric forcing data derived from observations or atmospheric analysis, the E3SM simulated atmospheric forcings are more uncertain (Hersbach et al., 2020). Atmospheric forcing has critical impacts on the flood simulation (Cloke and Pappenberger, 2009; Hjelmstad et al., 2021). The water movement in terrestrial and aquatic environments during a TC is strongly influenced by the TC's track and intensity (Pappenberger et al., 2005; Zhong et al., 2010). The uncertainty originating from atmospheric forcings would propagate to land, river, and ocean components through the multi-component framework (Deb et al., 2023; Blanton et al., 2020). Likewise, the hydrological uncertainties in the land and river components (Giuntoli et al., 2018; Feng et al., 2023) and the new coupling schemes (Feng et al., 2024) can also propagate and even amplify. Typically, the cascading meteorological uncertainty is handled by the ensemble approach (Hamill et al., 2011; Villarini et al., 2019). Multiple realizations of a TC event with perturbed initial conditions and/or model physics represent a range of scenarios that evolve differently based on the dynamics of the models (Blanton et al., 2020). However, the cascading meteorological uncertainty has not been systematically considered for CF modeling (Xu et al., 2023). It remains unclear whether such uncertainty will amplify or diminish when constrained by the physical processes inherent in ESMs.

Furthermore, the cascading uncertainty changes with the variability and complexity of hydrological drivers represented in models, because these factors are critical for determining how precipitation is partitioned into runoff and infiltration. As rainfall initially infiltrates the soil, subsurface runoff moves slowly through the soil layers. When the rainfall intensity exceeds the soil's absorption capacity, saturation-excess water leads to surface runoff. The rate of infiltration, which determines the balance between surface and subsurface runoff, is influenced by soil properties, antecedent moisture conditions (AMC) (Ivancic and Shaw, 2015), and land cover types. The runoffs are then routed through river networks, resulting in high river discharge (Fig. 1) (Bevacqua et al., 2020). Understanding the hydrological drivers, including the sensitivity of flood responses to various hydrological conditions such as AMC and rainfall scenarios, is crucial (Tramblay et al., 2010). These factors provide key insights for predicting different flood scenarios (Miguez-Macho and Fan, 2012;

https://doi.org/10.5194/egusphere-2024-2785
Preprint. Discussion started: 24 September 2024

Schrapffer et al., 2020). In particular, AMC plays a critical role in the generation of peak runoff and modulating riverine flooding characteristics during heavy precipitation events (Berghuijs et al., 2019; Nanditha and Mishra, 2022). A saturated AMC can significantly amplify flood impacts compared to drier conditions. The relative importance of rainfall and AMC varies depending on the watershed area. Soil moisture becomes a more dominant factor in larger watersheds (Ran et al., 2022). However, the role of these hydrologic drivers in cascading uncertainties sourced from atmospheric forcing has not been thoroughly explored in the context of CF, partly due to the absence of a tightly coupled modeling system (Jalili Pirani and Najafi, 2020).

While some of the model structure uncertainties, such as mesh resolution, have been extensively discussed (Camacho et al., 2015; Feng et al., 2019; Willis et al., 2019), the uncertainty relevant to model coupling has rarely been explored because the coupling capabilities have only recently been developed. Questions are raised regarding the role of model coupling and the magnitude of related uncertainty compared to meteorological uncertainty, especially given the characteristic spatiotemporal scales invoked in land-river and river-ocean coupling. Addressing these questions is critical to refining the performance of interactively coupled Earth System Models (ESMs), which is essential for achieving a more comprehensive understanding of the complex interactions and uncertainties associated with CF simulations. Moreover, assessing the enhancements provided by the two-way coupling schemes sheds light on the application of these couplings in future scenarios.

The above-mentioned uncertainties are complicated but must be carefully evaluated for ESMs as they will be more frequently applied for CF simulations in the context of climate change. This study focuses on exploring and disentangling the atmospheric, hydrological, and coupling uncertainties of coastal CF modeling within the coupled E3SM framework. We first provide a comprehensive description of the physical processes during a TC-induced CF event. We then evaluate the model coupling uncertainties and the cascading meteorological uncertainty using a simulation ensemble of a specific TC event. Using the atmospheric ensemble as a basis, we generated an expanded ensemble to analyze the relative contributions of different hydrological drivers to CF and how these contributions affect the accuracy and reliability of CF simulations. Finally, various hydrological and meteorological scenarios are used to delineate a spectrum of plausible CF outcomes in the designated region.

2 Materials and Methodology

2.1 Model Configuration

This study uses a recently developed configuration of E3SMv2 (Feng et al., 2024) (hereafter "E3SM coastal configuration"), which integrates global atmospheric (EAM), land (ELM), river (MOSART), and ocean (MPAS-O) models (Fig. 2a), across different coastal-refined meshes to improve the E3SM's capability in modeling coastal processes. This configuration incorporates advanced features such as variable-resolution land and river meshes (Liao et al., 2022, 2023a, b), global tide model with wetting and drying schemes in the barotropic MPAS-O (Barton et al., 2022; Pal et al., 2023), and two-way land-river and river-ocean coupling schemes (Xu et al., 2022b; Feng et al., 2024). The novel two-way hydrological coupling

https://doi.org/10.5194/egusphere-2024-2785
Preprint. Discussion started: 24 September 2024

between land and river components enables E3SM to capture the infiltration of inundated river water in floodplains and, subsequently, the enhancement of subsurface runoff and evapotranspiration from saturated floodplain soils (Xu et al., 2022b). The two-way river-ocean coupling was developed for E3SM to better represent the dynamic interaction between rivers and oceans, especially during CF events (Feng et al., 2024). This new approach allows for an accurate representation of coastal backwater effects and the mutual influences of river discharge and ocean sea surface height (SSH), providing a more realistic assessment of CF hazard risks (Feng et al., 2022).

Using the E3SM coastal configuration, we first simulated Hurricane Irene, a TC event that occurred in August 2011 and had large flooding impacts across the Mid-Atlantic region (Fig. 2b). Irene led to significant riverine and coastal flooding in the Delaware River Basin (DRB) and Delaware River Estuary (DBE) due to concurrent intense precipitation and storm surge. Following Feng et al. (2024), an ensemble of 25 EAM simulations with perturbed model parameters were performed to reproduce Irene and associated meteorological outcomes (see Appendix A in Deb et al. (2024)). These "prerun" EAM simulations were then prescribed within E3SM to drive the land, river, and ocean components, which together are able to reproduce the TC characteristics, including the storm track and intensity, as well as the TC impacts on river streamflow and SSH as measured by USGS and NOAA gauges (Feng et al., 2024). Fluvial and coastal inundations are simulated in MOSART and MPAS-O, respectively. Here, the total simulated inundation extent of Irene is benchmarked against a 250-m resolution inundation extent dataset based on satellite imagery (Tellman et al., 2021). The dataset is aggregated onto the MOSART mesh for comparison. Within each MOSART cell, we compute the fraction of the observed inundation. The model performance is evaluated using flood metrics defined by Wing et al. (2017), including hit rate (HR), false rate (FR) and success index (SI)

$$HR = \frac{M_1B_1}{M_1B_1+M_0B_1}, \tag{1}$$

$$FR = \frac{M_1B_0}{M_1B_0+M_1B_1}, \tag{2}$$

$$SI = \frac{M_1B_1}{M_1B_1+M_0B_1+M_1B_0}, \tag{3}$$

where M and B are the pixels (or grid cells) from model simulations and benchmark data, respectively. The subscripts 1 and 0 represent wet (inundated) and dry cells, respectively. In our simulations, a wet cell is identified if the simulated inundation fraction is above a small threshold of 0.02.

2.2 Model Coupling Uncertainty

The model coupling uncertainty is evaluated using three experiments (Table 1). The first two experiments only integrate ELM and MOSART, while the third experiment interactively couples MPAS-O with MOSART. All experiments are driven by the same EAM ensemble atmospheric forcing. Coastal inundation from MPAS-O at 250-m resolution is aggregated onto the coarser MOSART mesh that has the resolution of ~5 km in DRB. Within each MOSART grid cell, the inundation fraction is determined by the percentage of MPAS-O cells with a simulated water depth over 1 m. This number is used to

https://doi.org/10.5194/egusphere-2024-2785
Preprint. Discussion started: 24 September 2024

reflect adjustments for the MPAS-O inland bottom elevation bias relative to the actual data. Whenever there is a discrepancy between the inundation area from MOSART and MPAS-O in their overlapped cells near the coastline, the MPAS-O inundation is considered more accurate and will be used. The MOSART and MPAS-O simulated inundation extent is first evaluated against the benchmark data to justify the necessity of considering both riverine and coastal flooding within the coupled ESM. We then compared the streamflow along the Delaware River mainstem and riverine inundation in DRB in terms of flood metrics among different experiments to demonstrate the uncertainty of two-way coupling. The comparison of riverine inundation between Experiments 1 and 2 and between Experiments 1 and 3 shows the uncertainty from two-way land-river and river-ocean coupling, respectively. The comparison of total inundation between Experiments 1 and 3 quantifies the uncertainty if the ocean component is neglected in the CF simulation.

Table 1 Numerical experiments for quantifying model coupling uncertainty.

Experiment #	Configuration	Flooding type
1	ELM → MOSART	riverine
2	ELM ↔ MOSART	riverine
3	ELM → MOSART ↔ MPAS-O	riverine & coastal

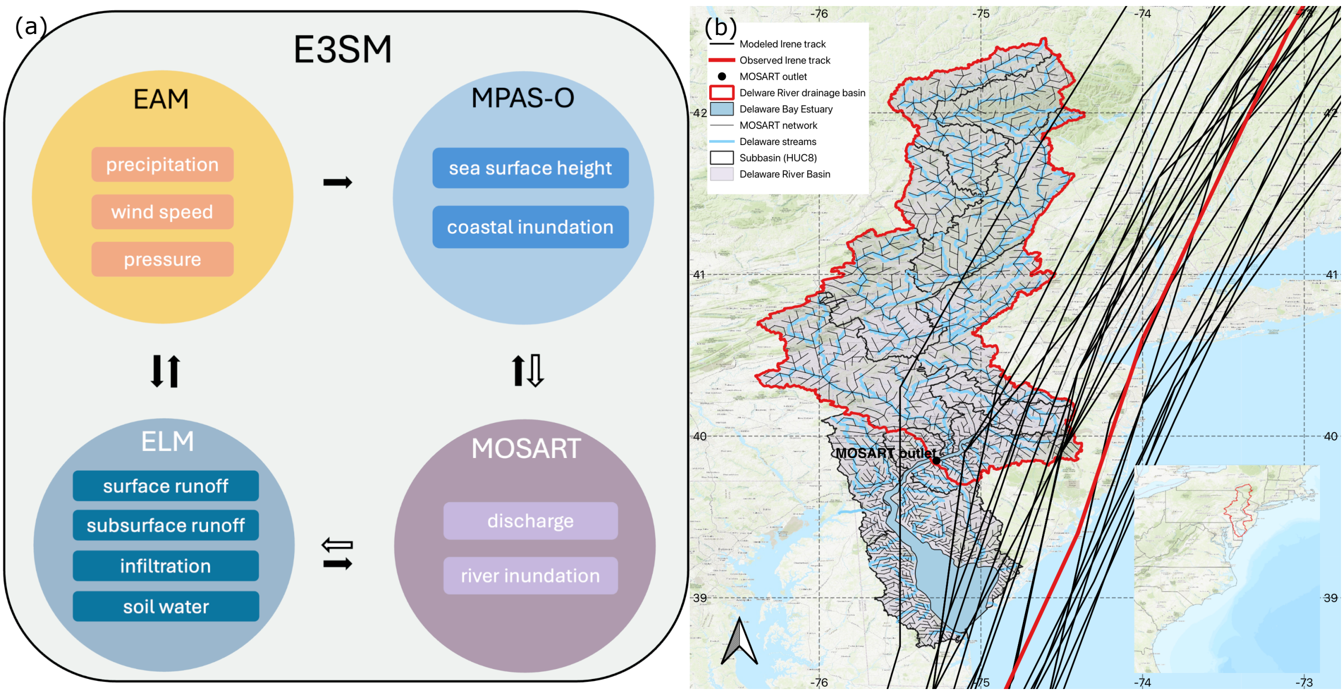

Figure 2: (a) The multi-component E3SM framework and drivers used for analyses within each model component. The black arrows represent the data flow via the one-way coupled framework. The white arrows are the new flow directions from the 2-way land-river and river-ocean models. (b) Map of Delaware river basin (DRB), Delaware bay estuary (DBE), and the observed (red) and modeled (black) Irene tracks. The topographic map in (b) is from the ESRI world topographic map (ESRI, 2012).

https://doi.org/10.5194/egusphere-2024-2785
Preprint. Discussion started: 24 September 2024

2.3 Cascading Meteorological Uncertainty

To understand the evolution of the meteorological uncertainty cascaded from atmospheric simulations through the multi-component framework, we applied the configuration of Experiment 3 (Table 1) and analyzed the interactions of those physically interconnected variables from the atmosphere, land, river, and ocean components of E3SM (Fig. 2a) including precipitation ($precip$), air pressure (P_{air}) and wind speed (U_{wind}) from EAM; surface runoff (Q_{sur}), subsurface runoff (Q_{sub}), infiltration (Q_{infl}) and soil water storage (Q_{soil}) from ELM; river discharge (Q) and riverine inundation area (A_{river}) from MOSART; SSH and coastal inundation area (A_{ocean}) from MPAS-O. The flux and state variables are represented by their event-accumulated and event-peak values within the Delaware River drainage basin, respectively (Fig. 2b). The estimated relationship between these variables represents the impact of one E3SM component on another component. For MOSART and MPAS-O, due to two-way river-ocean coupling, mutual relationships can occur between the related variables. The magnitude of uncertainty amplification or diminishment is quantified using normalized median absolute deviation (NMAD):

$$\mathrm{NMAD} = \frac{\mathrm{median}(|X_i - \mathrm{median}(X)|)}{\mathrm{median}(X)}, \tag{4}$$

and coefficient of variation (CV)

$$\mathrm{CV} = \frac{\sigma}{\mu}, \tag{5}$$

where X_i represents a variable X modeled at the ith ensemble run, and μ and σ are the mean and standard deviation of the corresponding variable computed from all ensemble simulations. These two metrics measure the spread of simulations with respect to the ensemble median and mean values separately.

Additionally, structural equation modeling (SEM) is applied as a path analysis method (Wright, 1921) to trace the flow of data and uncertainty. SEM estimates the complex relationships between two groups of variables by fitting multivariate regressions and uses the coefficient of a predictor to represent its contribution to the response variable. The Python library *semopy* is used in our SEM analyses (Igolkina and Meshcheryakov, 2020).

2.4 Uncertainty of Hydrological Drivers

The hydrological drivers we selected for uncertainty analysis include surface runoff, subsurface runoff, infiltration, and soil water storage. As the influence of these hydrological drivers shifts throughout a TC event due to changes in precipitation patterns, we chose to examine the cumulative impacts of these drivers across the entire event and track the temporal evolution of each driver's influence. For this purpose, we expand the original EAM simulation ensemble by introducing variations in AMC and runoff generation parameters within ELM. This expanded ensemble enables us to apply a machine learning approach to compute the permutation importance of each hydrological driver, providing insights into their roles in modulating flood risks. We focus exclusively on riverine flooding in this analysis. To avoid the substantial computational overhead associated with MPAS-O, we impose MPAS-O simulated water level as the coastal boundary condition of

https://doi.org/10.5194/egusphere-2024-2785
Preprint. Discussion started: 24 September 2024

MOSART (Feng et al., 2022). This approach represents the coastal backwater effects during CF, comparable to those obtained from the two-way river-ocean coupled configuration in Experiment 3 (Feng et al., 2024).

2.4.1 Expanded Ensemble simulation

The original EAM ensemble is expanded by first selecting 5 ensemble members that represent a reasonable spread of precipitation and then running each member with multiple AMC scenarios and different sets of runoff generation parameters. Five AMC scenarios were chosen to reflect a broad range of hydrological responses based on historical soil moisture trends, spanning from the driest to the wettest states. Specifically, we used the 0th, 25th, 50th, 75th and 100th percentiles of basin-averaged soil moisture during hurricane seasons from 2005 to 2011 as modeled in a historical ELM simulation (Fig. S1). The AMC at 75th percentile aligns with the observed AMC of Irene. Two parameters in ELM (f_{over} and f_{drain}, see Appendix A for a detailed definition) that determine the runoff generation are considered. Runoff is highly sensitive to both f_{over} and f_{drain}, which values usually have to be determined through sensitivity analysis. In the Mid-Atlantic region, as suggested by Xu et al. (2022a), we selected f_{over} values at 0.1, 0.5, 1, 2.5 and 5, and f_{drain} values at 2, 2.25, 2.5, 3 and 5. The peak discharge observed in the main channel of the Delaware River indicates that the impacts from changes in atmospheric conditions, AMC, and the parameters f_{over} and f_{drain} are widely distributed. These factors contribute to significant variations in the extent of riverine flooding. (Fig. S2~S5).

2.4.2 Quantifying Hydrological Driver Importance

To quantify the relative importance of each hydrological driver of CF, we employed a two-stage Artificial neural network (ANN) approach (Fig. 3). Compared to traditional regression models, ANN is particularly advantageous for capturing the complex, nonlinear relationships that exist between the diverse hydrological drivers and the resulting impacts on river systems (Goodfellow et al., 2016; LeCun et al., 2015; Tsang et al., 2017).

The first ANN model emulates the relationships between the hydrological drivers of Q_{sur}, Q_{sub}, Q_{infl} and Q_{soil} and perturbation parameters. Here, the input features are precipitation, AMC, f_{over} and f_{drain}, and the outputs are the aforementioned hydrological drivers. Then, these outputs become the input features for the second ANN, which emulates the relationships between river discharge and inundation area and these input features. To perform a detailed analysis, we first assessed the event-accumulated impacts of these drivers by aggregating data over the entire TC event. We also examined fine temporal impacts by using the second ANN on a daily basis. This allows us to understand not only the overall effect of each driver but also their day-to-day variations throughout the event. The relative importance of the input features on the output features is quantified using permutation importance. For more details about the ANN model setup and permutation importance calculation, please refer to Appendix B.

https://doi.org/10.5194/egusphere-2024-2785
Preprint. Discussion started: 24 September 2024

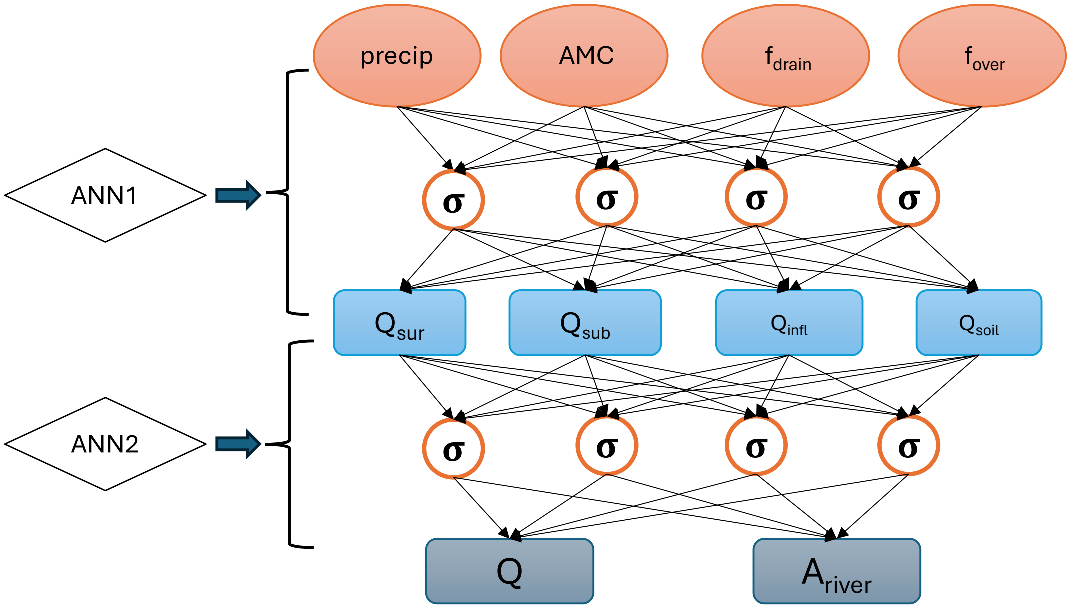

Figure 3: The densely connected ANNs for quantifying the relative importance of hydrological drivers to river discharge Q and inundation area A_{river}. Only 4 neurons per hidden layer are shown for illustration purposes. AMC refers to antecedent soil moisture condition.

3 Results

3.1 Model Coupling Uncertainty

The coastal configuration of E3SM (Experiment 3) effectively simulates compound riverine and coastal inundation through the coupled MOSART and MPAS-O models (Fig. 4). MOSART successfully predicts riverine flooding along the lower Delaware River and several upstream tributaries. However, it tends to overestimate the maximum extent of flooding along the Delaware River mainstem and some tributaries (Fig. 4a). Occasionally, some observed inundated cells in the upstream are captured by the model. Such bias is likely caused by the coarse spatial resolution of the river mesh, inaccurate river network delineation, and missing processes such as damming and flood defense constructions. Despite refinement, the mesh and river network still do not achieve the detail provided by regional high-resolution models (Dullo et al., 2021). More importantly, although MOSART is capable of simulating extensive riverine inundation in coastal regions, it cannot simulate the finer details of inundation immediately adjacent to the coastline (Fig. 4a), where coastal tide and storm surge play a significant role. To accurately represent these near-coastline inundations, it is essential to integrate MPAS-O (Fig. 4b), which is specifically designed to account for the dynamic interactions between tide and storm surge along the shoreline.

Comparison of flood metrics also confirms the importance of incorporating both riverine and coastal dynamics through a river-ocean coupled configuration (Fig. 5). Compared to Experiment 1 (Table 1) which does not activate MPAS-O, the river-ocean coupled configuration in Experiment 3 remarkably improves *HR* and *SI* by twofold with more than doubled the

https://doi.org/10.5194/egusphere-2024-2785
Preprint. Discussion started: 24 September 2024

predicted flooded area (FA) and reduces FR by ~0.1. The change in flood metrics implies that a significant portion (>70%) of the compound flooded area during Irene is accounted for by coastal flooding, which could be otherwise neglected if the ocean model is not coupled. However, the integration of MPAS-O does not reduce the MOSART-overpredicted flooded regions significantly, as suggested by the change of FR. It is nonetheless generally more prudent to overestimate rather than underestimate potential flooding from a flood hazard risk assessment perspective. These findings highlight the synergistic nature of river and ocean modeling in improving CF simulations in E3SM.

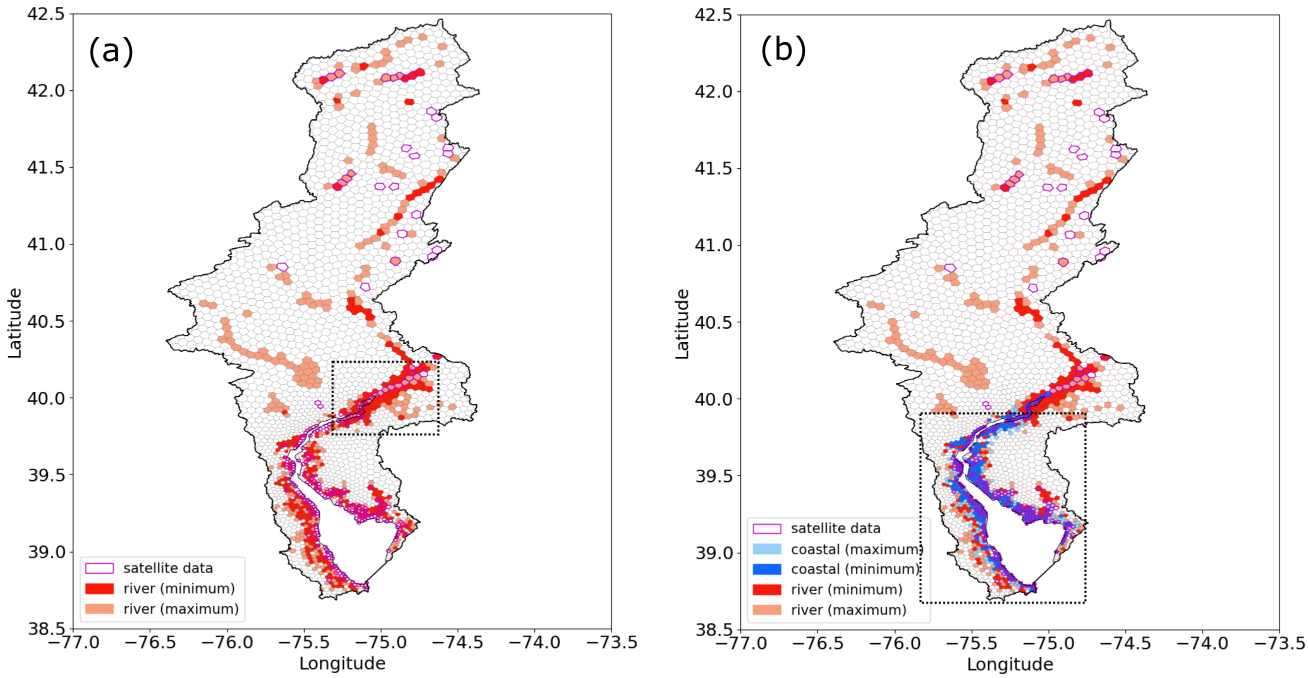

Figure 4: (a) MOSART simulated riverine inundation (red) against satellite-measured inundation (magenta box). The black dashed box highlights the lower Delaware River reach. (b) E3SM simulated riverine (red) and coastal (blue) total inundation against satellite data (magenta box). The black dashed box represents the coastline of DBE where extensive coastal inundation occurred. In both panels, dark and light colors represent the minimum and maximum inundated extent from the ensemble simulations, respectively.

https://doi.org/10.5194/egusphere-2024-2785
Preprint. Discussion started: 24 September 2024

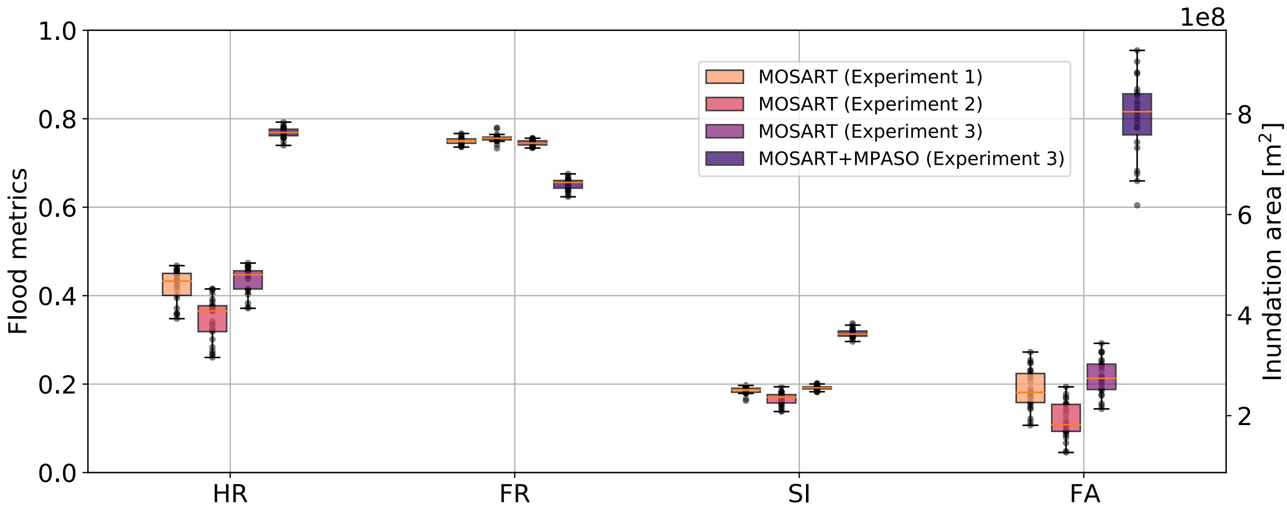

Figure 5: Flood metrics (*HR*, *FR*, *SI*) and flooded area (FA) used to compare riverine flooding in Experiments 1~3 and the combined riverine and coastal flooding in Experiment 3. Whiskers extend to 1.5 times the interquartile range from the quartile boundaries.

The comparison of Experiments 1~3 (Table 1) demonstrates the distinct role of land-river-ocean coupling in influencing CF (Fig. 6). Specifically, the implementation of two-way land-river coupling leads to a noticeable decrease in peak discharge along the Delaware River mainstem by 10~50 m^3/s which slightly increases towards the river outlet (Fig. 6a). Consequently, the simulated flooded area across the watershed is reduced in Experiment 2 compared to Experiment 1 (Fig. 6b). These reductions, despite being sporadic in upstream regions, are predominantly observed in the Lower Delaware River reach and near the coastline (Fig. 6b). This expected change is attributed to the two-way interaction of land and river hydrology implemented in Experiment 2, in which floodplain inundated water from MOSART is transferred to ELM, thereby reducing water storage within the channel and flood extent (Luo et al., 2017). Conversely, the influence of two-way river-ocean coupling (Experiment 3) appears to be mainly confined to the river reaches close to the outlet (Fig. 6c), where it significantly increases local streamflow (Fig. 6a). This is a result of more accurately representing the water and momentum fluxes between the river and ocean as well as coastal backwater effects. The elevated water levels due to tide and storm surge force an upstream propagation of ocean water into the river channel, leading to a subsequent increase in both river discharge and riverine flooded area in the low-lying regions (Feng et al., 2022).

https://doi.org/10.5194/egusphere-2024-2785
Preprint. Discussion started: 24 September 2024

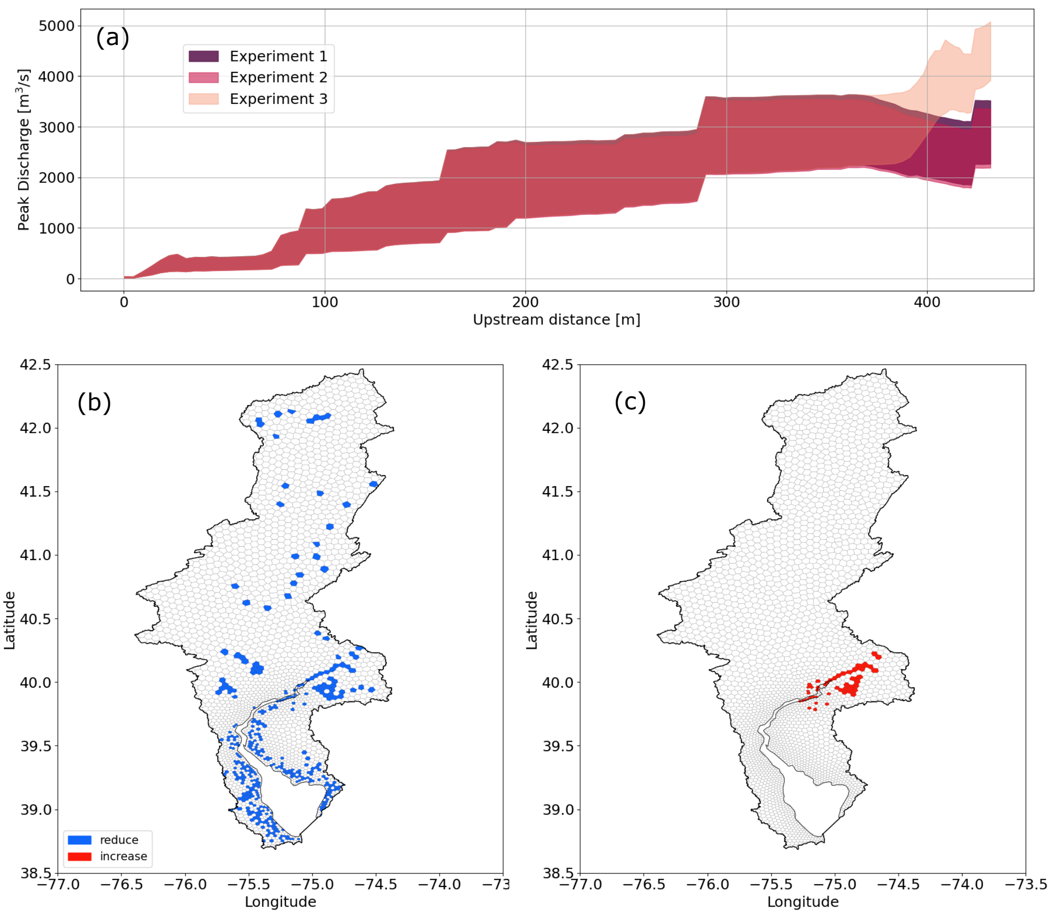

Figure 6: Comparison of flood impacts of model coupling. (a) Peak discharge along the Delaware River mainstem simulated by 1-way, 2-way land-river and river-ocean coupled simulations in Experiments 1, 2 and 3 (Table 1), respectively. Spatial maps of change in inundation of (b) two-way land river coupled simulations and (c) two-way river-ocean coupled simulations relative to 1-way coupled simulation in Figure 4a. Blue indicates reduced flooded area within the corresponding cell, while red implies an increase in flooded area.

The influence of the new two-way coupling schemes on the flood metrics is less significant than discharge, but insightful (Fig. 5). Comparing riverine flooding in Experiments 1 and 3, two-way river-ocean coupling improves the flood metrics by 0.01~0.02 and increases FA by ~2.5×10^7 m^2, as a result of a more accurate representation of backwater effects near the river outlet (Fig. 6c). Conversely, the two-way land-river coupling shows a slight reduction in flood metrics and FA, as also indicated in the spatial map (Fig. 6b). The discrepancies observed do not necessarily imply that the inclusion of land-river interactions compromises the results. Rather, they may result from the inherent uncertainties in both data and MOSART simulations, which tend to overestimate riverine flooding. The contrasting behaviors between the two coupling schemes primarily stem from their focus on different spatial and temporal scales. The two-way land-river coupling is crucial for capturing hydrological processes at larger spatiotemporal scales. However, building upon the macroscale inundation scheme in large-scale river models (Luo et al., 2017) potentially makes the coupling less reliable for event-scale riverine flooding.

https://doi.org/10.5194/egusphere-2024-2785
Preprint. Discussion started: 24 September 2024

The two-way river-ocean coupling is designed for accurately representing localized interactions between river discharge and tidal or storm surge dynamics that occur at diurnal or semi-diurnal scales. These findings highlight the complex interplay between various coupling approaches and the importance of tailored approaches in flood modeling to address specific hydrodynamic challenges effectively.

3.2 Cascading Meteorological Uncertainty

The SEM analysis depicts the possible pathways for the cascading propagation of meteorological and other uncertainties of CF simulations within E3SM (Fig. 7). Specifically, precipitation impacts runoff and infiltration nearly equally but it does not significantly influence soil water storage. The minimal variation in soil water during a TC event is likely because soil water storage cannot go above saturation. Runoff, which directly contributes to river discharge, positively affects flood simulation in terms of Q and A_{river} in MOSART. Conversely, the impact of infiltration and soil water storage on flooding is negative, as these processes reduce the surface runoff into river channels. Moreover, wind speed combined with air pressure affects sea level variations. The elevated sea level leads to an increase in the coastal inundation area. Additionally, there is a notable interaction between Q and SSH. Increased river discharge tends to elevate local SSH, while high SSH can impede river discharge (Dykstra and Dzwonkowski, 2020). This mutual interaction, frequently observed in CF events, underscores the complexity of the interactive processes influencing both riverine and coastal flooding dynamics, which need to be jointly considered in the two-way river-ocean coupled E3SM.

The cascading of meteorological uncertainty within the E3SM framework is assessed using CV and NMAD (Fig. 8). Both metrics suggest an amplification of meteorological uncertainty from atmospheric simulations throughout the multi-component system. In the context of riverine flooding, the variability among the ensemble for hydrological drivers such as surface runoff (Q_{sur}), subsurface runoff (Q_{sub}), and infiltration (Q_{infl}) is found to be comparable to that observed in precipitation. However, this variability escalates in riverine flood parameters, i.e., Q and A_{river}, where the CV and NMAD values are approximately twofold of those in precipitation. For coastal flooding, uncertainty increases from U_{wind} to SSH, which directly impacts coastal inundation levels (A_{ocean}). Much smaller uncertainty is presented in Q_{soil} and P_{air}. This analysis highlights the cascading nature of uncertainties from atmospheric inputs through meteorological and hydrological processes to final flood outcomes.

The analysis of the uncertainty path and propagation implies the critical role of hydrological drivers. By quantifying their relative contributions, we can better understand their roles in shaping the variability in riverine flooding outcomes, thereby refining the predictability of ESMs.

https://doi.org/10.5194/egusphere-2024-2785
Preprint. Discussion started: 24 September 2024

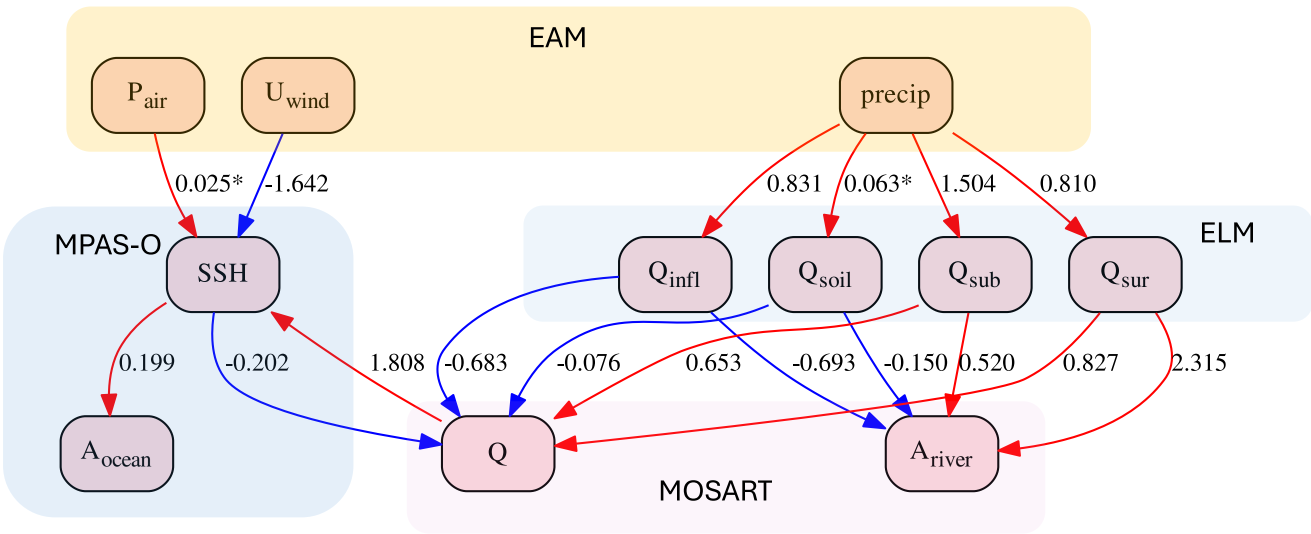

Figure 7: The structural equation model that describes the influence of variables on their response variables in EAM, ELM, MOSART and MPAS-O. Red and blue arrows show positive and negative influences, respectively. The asterisk sign implies the relationship is not significant with a p-value larger than 0.05.

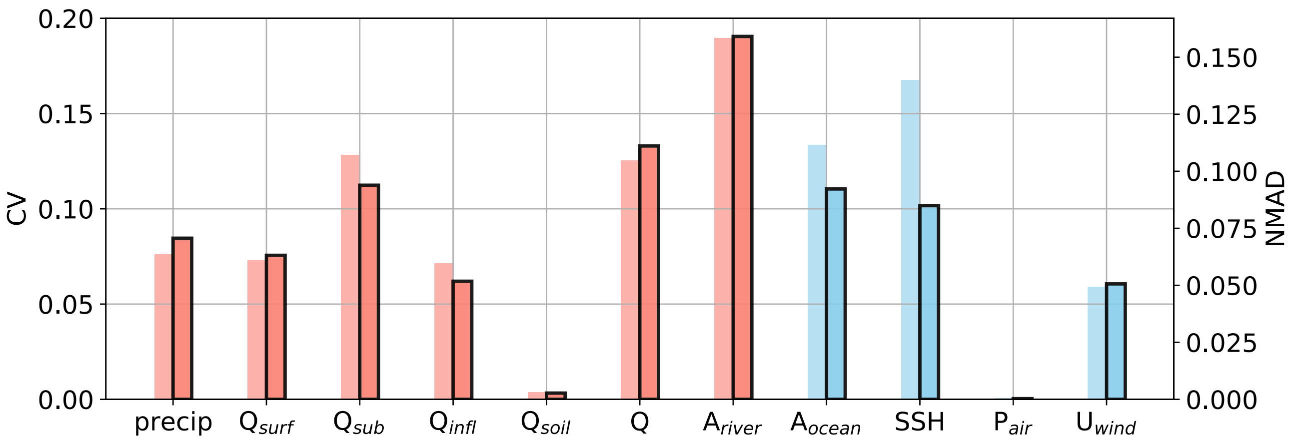

Figure 8: CV (light bars) and NMAD (dark bars with black margins) computed from the simulation ensembles for the variables selected in Section 2.3. Red and blue bars indicate riverine and coastal flood drivers, respectively.

3.3 Relative Importance of Hydrological Drivers

The extended ensemble simulations provide a wide range of scenarios, encompassing both lower and higher magnitudes of river discharge and riverine inundation compared to those observed during Hurricane Irene (Figure S6 and S7). The ANNs, trained from the ensemble output, achieve high skill scores. The r^2 and NRMSE values for the first ANN are 0.96 and 0.04, respectively, and are 0.97 and 0.03 for the second ANN.

https://doi.org/10.5194/egusphere-2024-2785
Preprint. Discussion started: 24 September 2024

Regarding the cumulative impacts over the entire Irene lifetime, the permutation importance derived from the first ANN highlights the crucial impact of AMC, f_{drain} and f_{over} on Q_{sur}, Q_{sub}, Q_{infl} and Q_{soil}, respectively, whereas precipitation shows more evenly distributed impacts on all the drivers (Fig. 9a). It should be noted that the relatively lower permutation importance values for precipitation do not suggest it is less important compared to the other factors. Rather, this is because in our ensemble, AMC, f_{drain} and f_{over} encompass a broader range of scenarios, whereas precipitation is from the Irene ensemble of simulations that only represent event-specific outcomes. The results of f_{drain} and f_{over} align well with their definitions in ELM (Appendix A), as f_{drain} and f_{over} dominate the change in Q_{sub} and Q_{sur}, respectively. Precipitation affects Q_{sur}, Q_{sub} and Q_{infl} nearly equally, which corresponds to their similar response presented in Figure 7.

The second ANN analyzes the impact of hydrological drivers on riverine flooding, i.e. river discharge (Q) and flooded area (A_{river}) (Fig. 9b). Our analysis demonstrates that Q_{sur} and Q_{sub} have similar influences on Q, whereas Q_{infl} shows a limited effect. In terms of A_{river}, Q_{sur} acts as the dominant factor, whereas Q_{sub} and Q_{infl} are less important but cannot be ignored. Q_{soil} has a minimal impact on both variables. The discrepancy between Q and A_{river} in their responses to these hydrological drivers can be attributed to the nature of the hydrology: river discharge is directly affected by surface and subsurface runoff, which are immediate responses to precipitation. In contrast, inundation across the river basin is more complex, as infiltration exerts a more localized effect and surface runoff may cause rapid flooding in response to intense rainfall. This differential impact implies the need for monitoring day-to-day variations in these drivers throughout the event to understand their dynamic role.

The time evolution of the permutation importance in the second ANN, trained on daily data during Hurricane Irene, illustrates the dynamic roles of hydrological drivers in response to the event and their contributions to riverine flooding. For river discharge, the influence of Q_{sur} and Q_{sub} varies notably before and during the peak flow (Fig. 10). Specifically, peak discharge was observed on August 30 at the river outlet (see Fig 15 in Feng et al., 2024), a period when Q_{sur} was predominant. In contrast, Q_{sub}, which typically contributes to baseflow, exerted more influence before the peak. Following the peak, the contributions of Q_{sur}, Q_{sub} and Q_{infl} leveled out as significant infiltration into the soil increased soil moisture, revealing a more significant effect of Q_{soil} than that seen in its event-cumulative impact (Fig. 9). The role of soil emerges as vital, acting as a buffer that modulates flooding during the heavy precipitation induced by the TC event. As the event progressed post-peak, there was a noticeable shift with a decreasing impact from Q_{sub} along with a bell-shaped variation in Q_{infl} and Q_{soil}. In terms of A_{river}, the dynamics slightly differ. Q_{sur} began dominating on August 28, two days earlier compared to Q, indicating the routing of discharge from the basin upstream to the outlet. These results reveal the importance of accurate runoff separation in the ESM framework for accurately modeling the time-varying nature of hydrological processes.

https://doi.org/10.5194/egusphere-2024-2785
Preprint. Discussion started: 24 September 2024

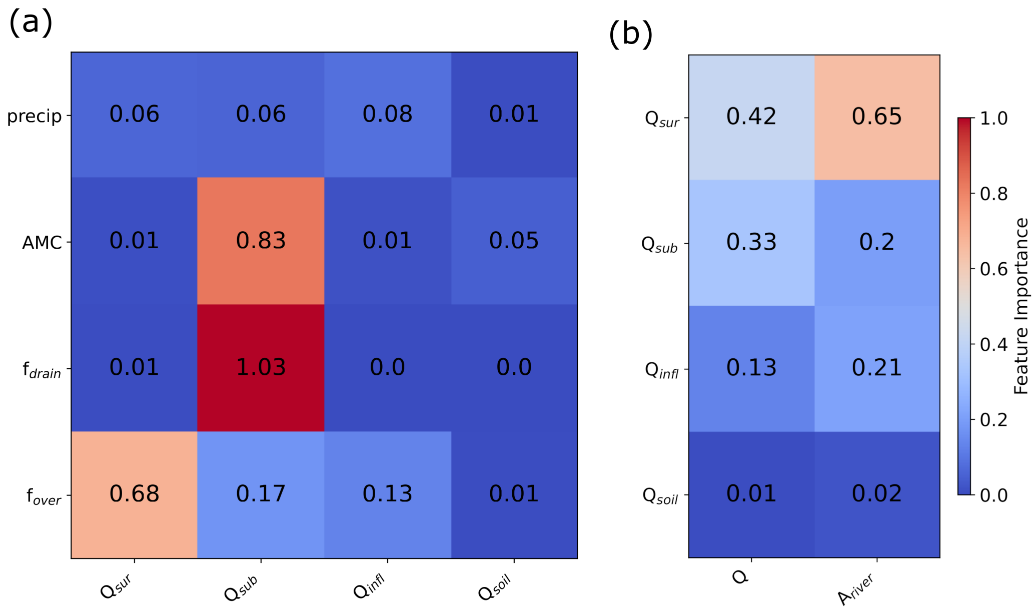

Figure 9: (a) Permutation importance of perturbation parameters (precipitation, AMC, f_{drain} *and* f_{over}) on hydrological drivers of Q_{sur}, Q_{sub}, Q_{infl} and Q_{soil}. The corresponding box plot of each driver is provided in row 1~4 of Figure S8. (b) Permutation importance of hydrological drivers on river discharge (Q) and flooded area (A_{river}). The scatter plots of Q and A_{river} against the drivers are respectively provided in the 5th and 6th rows of Figure S6.

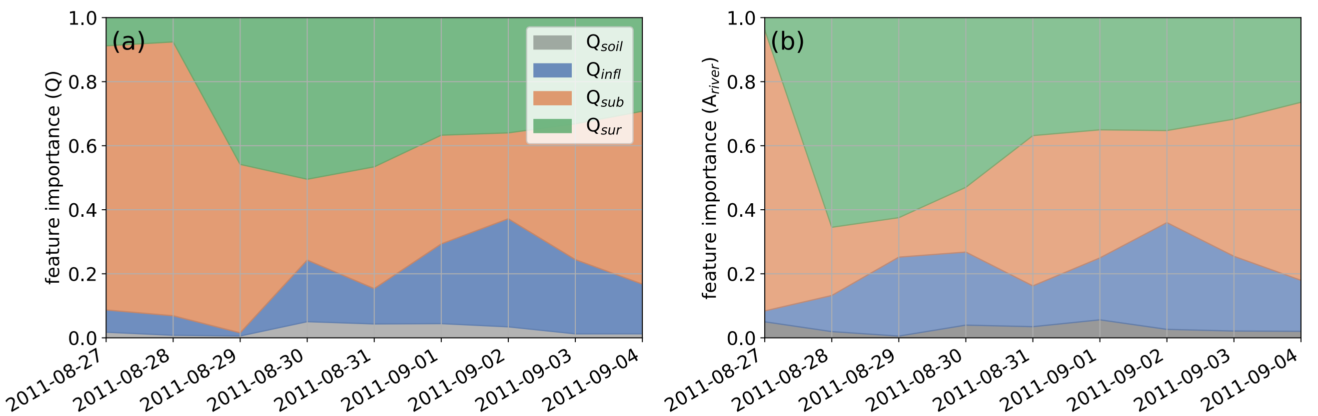

Figure 10: Time evolution of permutation importance (scaled between 0 and 1) of the four hydrological drivers for (a) Q and (b) A_{river}. The corresponding skill scores ($r^2$and NRMSE) of the ANNs trained using daily data are provided in Figure S9. The Irene-induced peak river discharge is on August 30, 2011.

4 Discussions

4.1 Uncertainties of CF simulations in E3SM

The integration of different coupling schemes into E3SM has large impacts on the simulated flooding. The exclusion of ocean coupling resulted in underestimations of the flood extent caused by tide and storm surges, critical for coastal flood assessments. Likewise, we showed that neglecting two-way land-river-ocean interactions distorted the modeled hydrological and hydrodynamic responses to the TC event, as the interactive mechanisms between terrestrial and aquatic systems were overlooked. Therefore, integrating comprehensive coupling mechanisms is essential for improving the predictability of ESMs, particularly in coastal regions vulnerable to complex, multivariate CF events. Additionally, we find that the uncertainty from the atmosphere simulations is comparable to that of two-way river-ocean coupling (i.e., the difference in riverine inundation modeled in Experiments 1 and 3), but is considerably smaller than the uncertainty of two-way river-ocean coupling if the MPAS-O modeled inundation is excluded (i.e., the difference in the combined riverine and coastal inundation between Experiments 1 and 3) (Fig. 5). The value of σ in Experiment 3 is 0.015, 0.014, 0.01 and 8.5×10^7 m^2 for HR, FR, SI and FA, respectively. This implies the critical need to account for the meteorological uncertainty and its cascading effects through the coupled system.

The complexities and inherent variabilities of hydrological drivers significantly influence flood risks through their interactions with meteorological conditions. Particularly, the soil's ability to buffer flood water crucially impacts the onset and development of floods (Fig. 10) (Blöschl, 2022). Predicting these effects remains challenging, primarily due to the spatial variability of soil characteristics and the spatiotemporal unpredictability of precipitation, such as shifting storm tracks and fluctuating intensity. This uncertainty is further compounded by key hydrological parameters in the land surface model. These parameters affect both the intensity and extent of runoff-driven inundation as well as the soil's response to moisture (Fig. 9). To address these challenges, CF modeling requires detailed land surface data and advanced modeling techniques, such as the incorporation of lateral flow (Han et al., 2024) and enhanced land-ocean and land-atmosphere coupling (Lin et al., 2023; Xu et al., 2024), to accurately simulate the interplay between atmospheric, land and river processes.

As discussed above, unlike single-driver flooding that can be simulated in isolated system components, the simulation of CF needs multi-component models, such as E3SM, which are capable of representing the compounding nature among drivers. However, this also introduces layers of additional uncertainties, particularly in the integration and interaction of model components (Jafarzadegan et al., 2023). Moreover, while regional models often focus on uncertainties arising from prescribed input forcings (Abbaszadeh et al., 2024; Muñoz et al., 2024), the uncertainties in ESMs can propagate bidirectionally through the coupled framework facilitated by two-way coupling schemes, which highlights the contrast in how uncertainties are generated and managed between regional models and ESMs. Quantifying these uncertainties within an integrated framework is crucial for advancing our understanding of CF but remains a formidable challenge. It necessitates a comprehensive examination of atmospheric, hydrological, oceanic and coupling uncertainties, a task that extends well beyond the capabilities of single-component models.

https://doi.org/10.5194/egusphere-2024-2785
Preprint. Discussion started: 24 September 2024

4.2 Definition of "Compound" Flooding

While previous CF studies predominantly focus on the contributions of high discharge, direct runoff, and precipitation to riverine flooding, our analysis reveals the underappreciated roles of other hydrological factors–particularly infiltration and AMC–in the context of CF. These factors significantly influence the flood dynamics in response to TC events. Specifically, we demonstrate that the concurrent occurrence of wet AMC with other CF drivers is not typically accounted for, implying a critical gap in the current CF definition. To capture a broad spectrum of plausible riverine flooding outcomes under varying simulated Irene tracks and AMC conditions, we extracted simulations from the expanded ensemble run by maintaining the default values for f_{drain} and f_{over}, resulting in 25 diverse scenarios. These scenarios suggest that a TC preceded by a wet AMC could drastically escalate flood risks. Notably, in all AMC scenarios, we observed a general increase in Q and A_{river} corresponding to increasing precipitation in DRB (Fig. 11a and 11b).

The variability within these simulations shows that the highest discharge was approximately 47% greater than the lowest discharge and 32% higher than during Irene itself (Fig. 11a). Moreover, in the worst-case inundation scenario, flooded areas could increase to more than twice (~2.4) of the flooded areas in the best scenario and the actual Irene event (Fig. 11b). Interestingly, the modeled inundation area for Irene closely aligns with the best-case scenario (Fig. 11b and 11c), indicating potentially greater risks if such events were to occur under much wetter AMC conditions. More alarmingly, the expansion of maximum inundation extent from Irene predominantly affects low-lying areas (Fig. 11c), increasing risks to coastal residents and highlighting the challenges in modeling complex river-ocean interactions, especially considering the effect of sea level rise. These findings suggest a broader definition of CF is needed. Similar to rain-on-snow flooding that may be classified as one type of CF (Zarzycki et al., 2024), a "compounding" event should also consider the co-occurrence of TCs and hydrological extremes, such as AMC, as high AMC can significantly amplify the TC flood impacts.

https://doi.org/10.5194/egusphere-2024-2785
Preprint. Discussion started: 24 September 2024

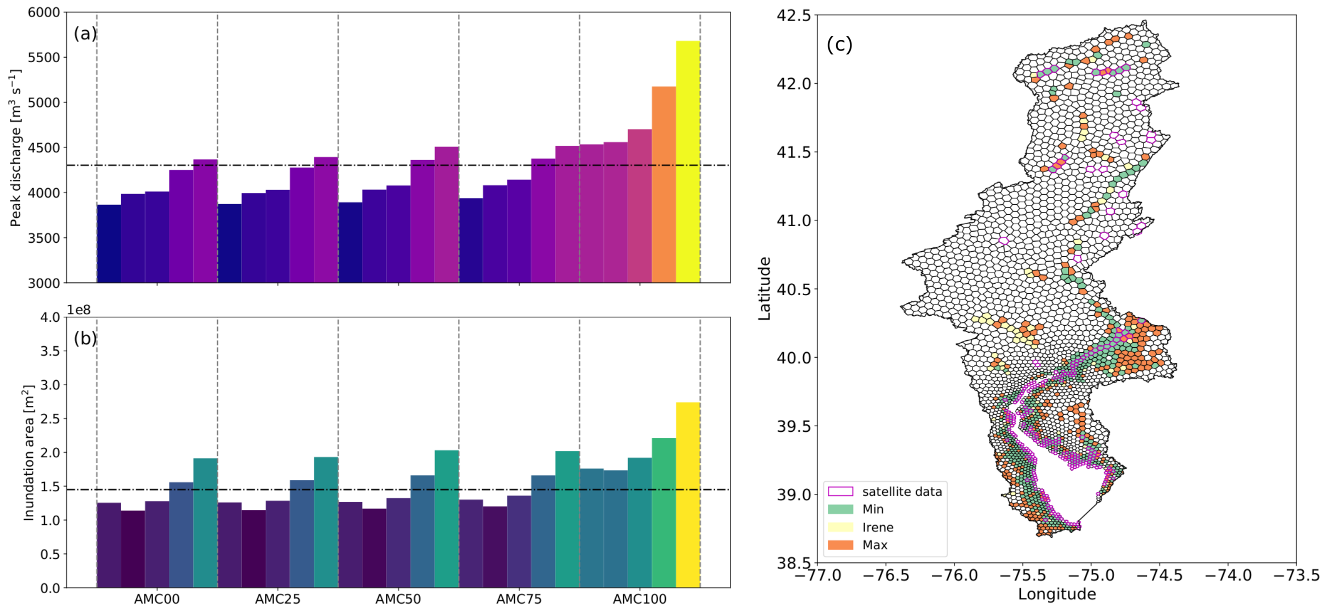

Figure 11: (a) Peak discharge and (b) riverine inundation area of 25 ensemble simulations. For each AMC, the ensemble runs are sequentially from EAM runs selected in Section 2.4.1. The dashed lines represent the results of the simulation that best describes Irene. (c) The plausible outcomes of inundated extent in DRB with the three colors representing the minimum (best-case scenario), Irene and maximum (worst-case scenario) inundation from the 25 ensemble runs.

4.3 Application of Advanced ESMs in Multivariate Flood Simulations

The application of E3SM in multivariate flood simulations brings a unique set of capabilities, especially when compared to fine-scale regional models. E3SM, with its ability to simulate interactions across various earth system components–atmosphere, land, river and ocean–offers a robust framework for understanding cross-scale environmental dynamics. Even with regional refinement, E3SM may still not be able to provide the street-level details of flood inundation because of missing processes (e.g., pluval inundation) and computational constraints. Although such capability is often crucial for urban planning and local flood risk management, large-scale E3SM has distinct advantages for broader application scopes. The efficiency in runtime makes it particularly suitable for disentangling interconnected drivers of complex physical processes and their cascading effects within an integrated framework. This efficiency is crucial for running multiple-scenario ensembles, which is essential for understanding the impacts of variability from physical drivers and climate change over extended periods, making it possible to simulate interactions like the newly developed two-way coupling between land, river and ocean. Although in Section 3.1 our analysis indicates that the land-river two-way coupling has relatively low impacts in short-term modeling of scenarios, its significance could increase in long-term climate simulations where gradual environmental changes play a more prominent role. Furthermore, E3SM provides the potential for climate change simulations, where the interactions of multiple planetary systems need to be considered over global scales and decadal to centennial timescales.

https://doi.org/10.5194/egusphere-2024-2785
Preprint. Discussion started: 24 September 2024

4.4 Limitations and Future Work

Despite these strengths, there are inherent challenges and potential sources of uncertainty in using E3SM for flood simulations. These uncertainties can stem from the models' resolution, numerical methods, the accuracy of input data, and the parameterization of complex hydrological and meteorological processes.

One limitation of this study is the exclusion of the ocean model in the expanded ensemble simulations, primarily due to the high computational costs associated with running the global MPAS-O. Future work may focus on developing a regional ocean model within the E3SM framework to enhance the efficiency and feasibility of these simulations. Currently, MPAS-O is geared towards global simulations, but adapting it for regional use could allow for more detailed and locally relevant flood simulations, integrating two-way land-ocean coupling to account for ocean water intrusion and its effect on soil moisture along coastlines. This is particularly relevant given our findings on the significant role of soil moisture in the context of TC-induced flooding.

Another avenue for future research involves conducting long-term climate change simulations to assess the impact of climatic drivers on CF dynamics. The existing long-term atmospheric forcing dataset does not adequately capture extreme TC events (Feng et al., 2024). Alternatively, employing a storyline approach (Pettett and Zarzycki, 2023) for event-specific studies could offer a more nuanced and scenario-based method to explore these extreme events and their interactions with other environmental drivers. This approach would not only enhance our understanding of climatic impacts on flooding but also improve the strategic planning and management of flood risks in vulnerable regions.

Our study demonstrates that parameters in runoff generation (i.e., f_{drain} and f_{over}) significantly influence river discharge and inundation (Fig. S4 and S5). When these parameters are considered alongside uncertainties in AMC and precipitation, the variability in flood outcomes expands considerably (Fig. S6 and S7). This broader range of variability exceeds that shown in Figure 11, indicating complex interactions between soil properties and hydrological responses. Given the critical global variability of soil properties, as indicated by the spatial distribution of f_{drain} and f_{over} in Xu et al. (2022a), we anticipate a greater variability in CF impacts that are dependent on soil conditions and land cover (Tran et al., 2024), in addition to topography (Feng et al., 2023). Furthermore, impervious surfaces, which are prevalent in coastal urban areas, may alter local runoff generation parameters (Zhang et al., 2018). This suggests that these parameters might require high-resolution representation in ELM to accurately reflect their spatial heterogeneity and to better represent urban areas (Li et al. 2024). Future work should focus on refining the spatial resolution in models to better capture the heterogeneity of soil and urban properties. This improvement could lead to more accurate simulations of how different land surface conditions affect flood dynamics, particularly in diverse geographic settings.

7 Conclusions

This study leverages the advanced capabilities of E3SM to improve our understanding of compound river and coastal flooding, highlighting the dynamic interaction between hydrological, riverine and coastal processes. Our research

https://doi.org/10.5194/egusphere-2024-2785
Preprint. Discussion started: 24 September 2024

demonstrates that an integrated atmosphere, land, river and ocean system significantly enhances the accuracy of multivariate flood modeling, capturing the cascade of uncertainties through the multi-component framework. The findings emphasize the significant influence of hydrological drivers, which can dramatically intensify the impacts of TC-driven flooding. This study not only showcases the robustness of E3SM in bridging gaps in current modeling approaches but also proposes a broader definition of CF that incorporates concurrent hydrological extremes. The implications of our research are profound, advocating for the inclusion of advanced, integrated modeling frameworks in future climate impact assessments to better predict and mitigate the risks of severe flooding events.

Appendix A: Runoff Generation Parameters in ELM

This section provides the definitions for the runoff generation parameters f_{over} and f_{drain} in ELM. The fraction of precipitation reaching the ground (Q_{liq}) that generates surface runoff (Q_{sur}) is determined by the saturation fraction (f_{sat}) of the grid cell:

$$Q_{sur} = f_{sat} Q_{liq}, \tag{A1}$$

$$f_{sat} = f_{max} exp\,(-0.5 f_{over} z_{\nabla}), \tag{A2}$$

where f_{max} is the potential or maximum saturation fraction of a grid cell, z_{∇} is the water table depth, and f_{over} is a decay factor for surface runoff (Niu et al., 2005). The subsurface runoff is parameterized as an exponential function of z_{∇}

$$Q_{sub} = \Theta_{ice} Q_{sub,max} exp\,(-f_{drain} z_{\nabla}), \tag{A3}$$

where Θ_{ice} is the ice impedance factor, $Q_{sub,max}$ is the maximum drainage rate, and f_{drain} is a decay factor.

Appendix B: ANN and Permutation Importance

In our setup, each ANN model included a hidden layer comprising 64 neurons, optimized using an adaptive optimization algorithm, Adam optimizer (Kingma and Ba, 2014). We selected mean square error (MSE) as the loss function to effectively measure the accuracy of predictions during training, which was conducted in the deep learning platform TensorFlow (Abadi et al., 2016). The model completed 600 epochs with a batch size of 32 to ensure thorough learning and convergence. Before training, the data were split into training and testing datasets, and each variable is normalized with respect to its maxima. The ANN performance was evaluated on the testing dataset using coefficient of determination (r^2) and normalized root mean squared error (NRMSE).

Despite the high accuracy achieved by ANN models, it can be challenging to pinpoint the specific influence of individual input variables on output variables (Pires dos Santos et al., 2019). Herein, we employed permutation importance to measure the relative significance of input features within complex ANN models. Permutation importance is a technique used to evaluate the importance of features in a predictive model (Fisher et al., 2019). It assesses the impact of each feature on the model's performance by measuring how much the model's performance decreases when the values of that feature are randomly permuted while leaving other features unchanged (Štrumbelj and Kononenko, 2014; Shrikumar et al., 2017). This method allows quantifying how variations in a single input feature can affect a particular output or overall predictive accuracy. In this study, we computed permutation importance using SHAP (Shapley Additive Explanations, (Lundberg and Lee, 2017)) on the test dataset.

Code and data availability.

All model simulations will be uploaded to Zenodo as an open repository upon acceptance.

Author contributions.

DF and ZT designed the methodology and the numerical experiments. DE, JW, DX, CL, GB and JB prepared the unstructured global meshes, MOSART river networks, model parameter files and EAM ensemble simulations. DF carried out the analysis and the result visualization. DF and ZT wrote the initial draft of the manuscript. All authors contributed to the discussion and review of the results and to the editing of the paper.

Competing interests

The contact author has declared that none of the authors has any competing interests.

Acknowledgement.

This research has been supported by the Earth System Model Development program areas of the U.S. Department of Energy, Office of Science, Office of Biological and Environmental Research as part of the multi-program, collaborative Integrated Coastal Modeling (ICoM) project (grant no. KP1703110/75415). H.-Y. Li was also supported by the Earth and Environmental Systems Sciences Division of the U.S. Department of Energy, Office of Science, Office of Biological and Environmental Research as part of the project “A strategic partnership between the College of Engineering at University of Houston and Pacific Northwest National Lab” (grant no. DE-SC0023295). All model simulations were performed using resources available through (a) Research Computing at Pacific Northwest National Laboratory (PNNL) and (b) the National Energy Research Scientific Computing Center (NERSC), a U.S. Department of Energy Office of Science User Facility located at Lawrence Berkeley National Laboratory, operated under Contract No. DE-AC02-05CH11231 using NERSC award BER-ERCAP0027647. PNNL is operated for DOE by Battelle Memorial Institute, United States, under contract DE-AC05-76RL01830.

References

Abadi, M., Barham, P., Chen, J., Chen, Z., Davis, A., Dean, J., Devin, M., Ghemawat, S., Irving, G., Isard, M., et al.: Tensorflow: A system for large-scale machine learning, in: 12th USENIX symposium on operating systems design and implementation (OSDI 16), pp. 265–283, 415 ISBN 978-1-931971-33-1, 2016.

Abbaszadeh, P., Munoz, D. F., Moftakhari, H., Jafarzadegan, K., and Moradkhani, H.: Perspective on uncertainty quantification and reduction in compound flood modeling and forecasting, Iscience, 25, 10.1016/j.isci.2022.105201, 2022.

Barton, K. N., Pal, N., Brus, S. R., Petersen, M. R., Arbic, B. K., Engwirda, D., Roberts, A. F., Westerink, J. J., Wirasaet, D., and Schindelegger, M.: Global Barotropic Tide Modeling Using Inline Self-Attraction and Loading in MPAS-Ocean, Journal of Advances in Modeling Earth Systems, 14, e2022MS003207, https://doi.org/10.1029/2022MS003207, 2022.

Bates, P. D., Quinn, N., Sampson, C., Smith, A., Wing, O., Sosa, J., Savage, J., Olcese, G., Neal, J., Schumann, G., et al.: Combined modelling of US fluvial, pluvial, and coastal flood hazard under current and future climates, Water Resources Research, 57, e2020WR028673, https://doi.org/10.1029/2020WR028673, 2021.

Berghuijs, W. R., Harrigan, S., Molnar, P., Slater, L. J., and Kirchner, J. W.: The relative importance of different flood-generating mechanisms across Europe, Water Resources Research, 55, 4582–4593, https://doi.org/10.1029/2019WR024841, 2019.

Bevacqua, E., Vousdoukas, M. I., Zappa, G., Hodges, K., Shepherd, T. G., Maraun, D., Mentaschi, L., and Feyen, L.: More meteorological events that drive compound coastal flooding are projected under climate change, Communications earth & environment, 1, 47, https://doi.org/10.1038/s43247-020-00044-z, 2020.

Bilskie, M. and Hagen, S.: Defining flood zone transitions in low-gradient coastal regions, Geophysical Research Letters, 45, 2761–2770, https://doi.org/10.1002/2018GL077524, 2018.

Blanton, B., Dresback, K., Colle, B., Kolar, R., Vergara, H., Hong, Y., Leonardo, N., Davidson, R., Nozick, L., and Wachtendorf, T.: An Integrated Scenario Ensemble-Based Framework for Hurricane Evacuation Modeling: Part 2—Hazard Modeling, Risk analysis, 40, 117– 133, https://doi.org/10.1111/risa.13004, 2020.

Blöschl, G.: Three hypotheses on changing river flood hazards, Hydrology and Earth System Sciences, 26, 5015-5033, 10.5194/hess-26-5015-2022, 2022.

Camacho, R. A., Martin, J. L., McAnally, W., Díaz-Ramirez, J., Rodriguez, H., Sucsy, P., and Zhang, S.: A comparison of Bayesian methods for uncertainty analysis in hydraulic and hydrodynamic modeling, JAWRA Journal of the American Water Resources Association, 51, 1372–1393, https://doi.org/10.1111/1752-1688.12319, 2015.

Costabile, P., Costanzo, C., Kalogiros, J., and Bellos, V.: Toward street-level nowcasting of flash floods impacts based on HPC hydrodynamic modeling at the watershed scale and high-resolution weather radar data, Water Resources Research, 59, e2023WR034599, 10.1029/2023WR034599, 2023.

Cloke, H. L. and Pappenberger, F.: Ensemble flood forecasting: A review, Journal of hydrology, 375, 613-626, 10.1016/j.jhydrol.2009.06.005, 2009.

https://doi.org/10.5194/egusphere-2024-2785
Preprint. Discussion started: 24 September 2024

Deb, M., Benedict, J. J., Sun, N., Yang, Z., Hetland, R. D., Judi, D., and Wang, T.: Estuarine hurricane wind can intensify surge-dominated extreme water level in shallow and converging coastal systems, Natural Hazards and Earth System Sciences, 24, 2461-2479, 10.5194/nhess-24-2461-2024, 2024.

Dullo, T. T., Gangrade, S., Morales-Hernández, M., Sharif, M. B., Kao, S.-C., Kalyanapu, A. J., Ghafoor, S., and Evans, K. J.: Simulation of Hurricane Harvey flood event through coupled hydrologic-hydraulic models: Challenges and next steps, Journal of Flood Risk Management, 14, e12716, https://doi.org/10.1111/jfr3.12716, 2021.

Dykstra, S. and Dzwonkowski, B.: The propagation of fluvial flood waves through a backwater-estuarine environment, Water Resources Research, 56, e2019WR025743, https://doi.org/10.1029/2019WR025743, 2020.

ESRI. "Topographic" [basemap]. Scale Not Given. "World Topographic Map". http://www.arcgis.com/home/item.html?id=30e5fe3149c34df1ba922e6f5bbf808f, last access: 23 September 2024, 2012.

Feng, D., Passalacqua, P., and Hodges, B. R.: Innovative approaches for geometric uncertainty quantification in an operational oil spill modeling system, Journal of Marine Science and Engineering, 7, 259, https://doi.org/10.3390/jmse7080259, 2019.

Feng, D., Tan, Z., Engwirda, D., Liao, C., Xu, D., Bisht, G., Zhou, T., Li, H.-Y., and Leung, L. R.: Investigating coastal backwater effects and flooding in the coastal zone using a global river transport model on an unstructured mesh, Hydrology and Earth System Sciences, 26, 5473–5491, https://doi.org/10.5194/hess-26-5473-2022, 2022.

Feng, D., Tan, Z., Xu, D., and Leung, L. R.: Understanding the compound flood risk along the coast of the contiguous United States, Hydrology and Earth System Sciences, 27, 3911–3934, https://doi.org/10.5194/hess-27-3911-2023, 2023.

Feng, D., Tan, Z., Engwirda, D., Wolfe, J. D., Xu, D., Liao, C., Bisht, G., Benedict, J. J., Zhou, T., Li, H.-Y., et al.: Simulation of compound flooding using river-ocean two-way coupled E3SM ensemble on variable-resolution meshes, Journal of Advances in Modeling Earth Systems, 16, e2023MS004054, https://doi.org/10.1029/2023MS004054, 2024.

Fisher, A., Rudin, C., and Dominici, F.: All models are wrong, but many are useful: Learning a variable's importance by studying an entire class of prediction models simultaneously, Journal of Machine Learning Research, 20, 1–81, 2019.

Giuntoli, I., Villarini, G., Prudhomme, C., and Hannah, D. M.: Uncertainties in projected runoff over the conterminous United States, Climatic change, 150, 149–162, https://doi.org/10.1007/s10584-018-2280-5, 2018.

Golaz, J.-C., Caldwell, P. M., Van Roekel, L. P., Petersen, M. R., Tang, Q., Wolfe, J. D., Abeshu, G., Anantharaj, V., Asay-Davis, X. S., Bader, D. C., et al.: The DOE E3SM coupled model version 1: Overview and evaluation at standard resolution, Journal of Advances in Modeling Earth Systems, 11, 2089–2129, https://doi.org/10.1029/2018MS001603, 2019.

Golaz, J.-C., Van Roekel, L. P., Zheng, X., Roberts, A. F., Wolfe, J. D., Lin, W., Bradley, A. M., Tang, Q., Maltrud, M. E., Forsyth, R. M., et al.: The DOE E3SM Model Version 2: overview of the physical model and initial model evaluation, Journal of Advances in Modeling Earth Systems, 14, https://doi.org/10.1029/2022MS003156, 2022.

Goodfellow, I., Bengio, Y., and Courville, A.: Deep learning, MIT press, ISBN 9780262035613, 2016.

Hamill, T. M., Whitaker, J. S., Kleist, D. T., Fiorino, M., and Benjamin, S. G.: Predictions of 2010's tropical cyclones using the GFS and ensemble-based data assimilation methods, Monthly Weather Review, 139, 3243–3247, https://doi.org/10.1175/MWR-D-11-00079.1, 2011.

Hjelmstad, A., Shrestha, A., Garcia, M., and Mascaro, G.: Propagation of radar rainfall uncertainties into urban pluvial flood modeling during the North American monsoon, Hydrological Sciences Journal, 66, 2232-2248, 10.1080/02626667.2021.1980216, 2021.

Qiu, H., Bisht, G., Li, L., Hao, D., and Xu, D.: Development of inter-grid-cell lateral unsaturated and saturated flow model in the E3SM Land Model (v2. 0), Geoscientific Model Development, 17, 143-167, 10.5194/gmd-17-143-2024, 2024.

Hendry, A., Haigh, I. D., Nicholls, R. J., Winter, H., Neal, R., Wahl, T., Joly-Laugel, A., and Darby, S. E.: Assessing the characteristics and drivers of compound flooding events around the UK coast, Hydrology and Earth System Sciences, 23, 3117–3139, https://doi.org/10.5194/hess-23-3117-2019, 2019.

Hersbach, H., Bell, B., Berrisford, P., Hirahara, S., Horányi, A., Muñoz-Sabater, J., Nicolas, J., Peubey, C., Radu, R., and Schepers, D.: The ERA5 global reanalysis, Quarterly Journal of the Royal Meteorological Society, 146, 1999-2049, 10.1002/qj.3803, 2020.

Igolkina, A. A. and Meshcheryakov, G.: semopy: A python package for structural equation modeling, Structural Equation Modeling: A 475 Multidisciplinary Journal, 27, 952–963, https://doi.org/10.1080/10705511.2019.1704289, 2020.

Ivancic, T. J. and Shaw, S. B.: Examining why trends in very heavy precipitation should not be mistaken for trends in very high river discharge, Climatic Change, 133, 681–693, https://doi.org/10.1007/s10584-015-1476-1, 2015.

Ivanov, V. Y., Xu, D., Dwelle, M. C., Sargsyan, K., Wright, D. B., Katopodes, N., Kim, J., Tran, V. N., Warnock, A., and Fatichi, S.: Breaking down the computational barriers to real-time urban flood forecasting, Geophysical Research Letters, 48, e2021GL093585, 10.1029/2021GL093585, 2021.

Jafarzadegan, K., Moradkhani, H., Pappenberger, F., Moftakhari, H., Bates, P., Abbaszadeh, P., Marsooli, R., Ferreira, C., Cloke, H. L., and Ogden, F.: Recent advances and new frontiers in riverine and coastal flood modeling, Reviews of Geophysics, 61, e2022RG000788, 10.1029/2022RG000788, 2023.

Jalili Pirani, F. and Najafi, M.: Recent trends in individual and multivariate compound flood drivers in Canada's coasts, Water Resources Research, 56, e2020WR027785, https://doi.org/10.1029/2020WR027785, 2020.

Kingma, D. P. and Ba, J.: Adam: A method for stochastic optimization, arXiv preprint arXiv:1412.6980, https://doi.org/10.48550/arXiv.1412.6980, 2014.

LeCun, Y., Bengio, Y., and Hinton, G.: Deep learning, nature, 521, 436–444, https://doi.org/10.1038/nature14539, 2015.

Leonard, M., Westra, S., Phatak, A., Lambert, M., van den Hurk, B., McInnes, K., Risbey, J., Schuster, S., Jakob, D., and Stafford-Smith, M.: A compound event framework for understanding extreme impacts, Wiley Interdisciplinary Reviews: Climate Change, 5, 113–128, https://doi.org/10.1002/wcc.252, 2014.

Li, D., Lettenmaier, D. P., Margulis, S. A., and Andreadis, K.: The role of rain-on-snow in flooding over the conterminous United States, 485 Water Resources Research, 55, 8492–8513, https://doi.org/10.1029/2019WR024950, 2019.

Liao, C., Zhou, T., Xu, D., Barnes, R., Bisht, G., Li, H.-Y., Tan, Z., Tesfa, T., Duan, Z., Engwirda, D., et al.: Advances in hexagon mesh-based flow direction modeling, Advances in Water Resources, 160, 104099, https://doi.org/10.1016/j.advwatres.2021.104099, 2022.

Liao, C., Zhou, T., Xu, D., Cooper, M. G., Engwirda, D., Li, H.-Y., and Leung, L. R.: Topological Relationship-Based Flow Direction Modeling: Mesh-Independent River Networks Representation, Journal of Advances in Modeling Earth Systems, 15, e2022MS003089, https://doi.org/10.1029/2022MS003089, 2023a.

Liao, C., Zhou, T., Xu, D., Tan, Z., Bisht, G., Cooper, M. G., Engwirda, D., Li, H.-Y., and Leung, L. R.: Topological Relationship-Based Flow Direction Modeling: Stream Burning and Depression Filling, Journal of Advances in Modeling Earth Systems, 15, e2022MS003487, https://doi.org/10.1029/2022MS003487, 2023b.

Lilly, J. R., Capodaglio, G., Petersen, M. R., Brus, S. R., Engwirda, D., and Higdon, R. L.: Storm Surge Modeling as an Application of Local Time-Stepping in MPAS-Ocean, Journal of Advances in Modeling Earth Systems, 15, e2022MS003327, https://doi.org/10.1029/2022MS003327, 2023.

Lin, G., Leung, L. R., Lee, J., Harrop, B. E., Baker, I. T., Branson, M. D., Denning, A. S., Jones, C. R., Ovchinnikov, M., and Randall, D. A.: Modeling Land-Atmosphere Coupling at Cloud-Resolving Scale Within the Multiple Atmosphere Multiple Land (MAML) Framework in SP-E3SM, Journal of Advances in Modeling Earth Systems, 15, e2022MS003101, 10.1029/2022MS003101, 2023.

Loveland, M., Kiaghadi, A., Dawson, C. N., Rifai, H. S., Misra, S., Mosser, H., and Parola, A.: Developing a modeling framework to simulate compound flooding: when storm surge interacts with riverine flow, Frontiers in Climate, 2, 609610, https://doi.org/10.3389/fclim.2020.609610, 2021.

Lundberg, S. M. and Lee, S.-I.: A Unified Approach to Interpreting Model Predictions, in: Advances in Neural Information Processing Systems 30, edited by Guyon, I., Luxburg, U. V., Bengio, S., Wallach, H., Fergus, R., Vishwanathan, S., and Garnett, R., pp. 4765–4774, Curran Associates, Inc., http://papers.nips.cc/paper/7062-a-unified-approach-to-interpreting-model-predictions.pdf, 2017.

Luo, X., Li, H.-Y., Leung, L. R., Tesfa, T. K., Getirana, A., Papa, F., and Hess, L. L.: Modeling surface water dynamics in the Amazon Basin using MOSART-Inundation v1. 0: impacts of geomorphological parameters and river flow representation, Geoscientific model 505 development, 10, 1233–1259, https://doi.org/10.5194/gmd-10-1233-2017, 2017.

Miguez-Macho, G. and Fan, Y.: The role of groundwater in the Amazon water cycle: 1. Influence on seasonal streamflow, flooding and wetlands, Journal of Geophysical Research: Atmospheres, 117, https://doi.org/10.1029/2012JD017539, 2012.

Moftakhari, H. R., Salvadori, G., AghaKouchak, A., Sanders, B. F., and Matthew, R. A.: Compounding effects of sea level rise and fluvial flooding, Proceedings of the National Academy of Sciences, 114, 9785–9790, https://doi.org/10.1073/pnas.1620325114, 2017.

Muñoz, D. F., Moftakhari, H., and Moradkhani, H.: Quantifying cascading uncertainty in compound flood modeling with linked process-based and machine learning models, Hydrology and Earth System Sciences, 28, 2531-2553, 10.5194/hess-28-2531-2024, 2024.

Nanditha, J. and Mishra, V.: Multiday precipitation is a prominent driver of floods in Indian river basins, Water Resources Research, 58, e2022WR032723, https://doi.org/10.1029/2022WR032723, 2022.

Niu, G.-Y., Yang, Z.-L., Dickinson, R. E., and Gulden, L. E.: A simple TOPMODEL-based runoff parameterization (SIMTOP) for use in 515 global climate models, Journal of Geophysical Research: Atmospheres, 110, https://doi.org/10.1029/2005JD006111, 2005.

Pal, N., Barton, K. N., Petersen, M. R., Brus, S. R., Engwirda, D., Arbic, B. K., Roberts, A. F., Westerink, J. J., and Wirasaet, D.: Barotropic tides in MPAS-Ocean (E3SM V2): impact of ice shelf cavities, Geoscientific Model Development, 16, 1297–1314, https://doi.org/10.5194/gmd-16-1297-2023, 2023.

Pappenberger, F., Beven, K. J., Hunter, N., Bates, P., Gouweleeuw, B. T., Thielen, J., and De Roo, A.: Cascading model uncertainty from medium range weather forecasts (10 days) through a rainfall-runoff model to flood inundation predictions within the European Flood Forecasting System (EFFS), Hydrology and Earth System Sciences, 9, 381–393, https://doi.org/10.5194/hess-9-381-2005, 2005.

Pettett, A. and Zarzycki, C. M.: The 1996 Mid-Atlantic Winter Flood: Exploring Climate Risk through a Storyline Approach, Journal of Hydrometeorology, 24, 2259-2280, 10.1175/JHM-D-22-0146.1, 2023.

Pires dos Santos, R., Dean, D., Weaver, J., and Hovanski, Y.: Identifying the relative importance of predictive variables in artificial neural networks based on data produced through a discrete event simulation of a manufacturing environment, International Journal of Modelling and Simulation, 39, 234–245, https://doi.org/10.1080/02286203.2018.1558736, 2019.

Ran, Q., Wang, J., Chen, X., Liu, L., Li, J., and Ye, S.: The relative importance of antecedent soil moisture and precipitation in flood generation in the middle and lower Yangtze River basin, Hydrology and Earth System Sciences, 26, 4919–4931, https://doi.org/10.5194/hess-264919-2022, 2022.

Santiago-Collazo, F. L., Bilskie, M. V., and Hagen, S. C.: A comprehensive review of compound inundation models in low-gradient coastal watersheds, Environmental Modelling & Software, 119, 166–181, https://doi.org/10.1016/j.envsoft.2019.06.002, 2019.

Sarhadi, A., Rousseau-Rizzi, R., Mandli, K., Neal, J., Wiper, M. P., Feldmann, M., and Emanuel, K.: Climate change contributions to increasing compound flooding risk in New York City, Bulletin of the American Meteorological Society, 105, E337–E356, https://doi.org/10.1175/BAMS-D-23-0177.1, 2024.

Schrapffer, A., Sörensson, A., Polcher, J., and Fita, L.: Benefits of representing floodplains in a Land Surface Model: Pantanal simulated with ORCHIDEE CMIP6 version, Climate Dynamics, 55, 1303–1323, https://doi.org/10.1007/s00382-020-05324-0, 2020.

Shrikumar, A., Greenside, P., and Kundaje, A.: Learning important features through propagating activation differences, in: International conference on machine learning, pp. 3145–3153, PMLR, 2017.

Štrumbelj, E. and Kononenko, I.: Explaining prediction models and individual predictions with feature contributions, Knowledge and information systems, 41, 647–665, https://doi.org/10.1007/s10115-013-0679-x, 2014.

Tellman, B., Sullivan, J. A., Kuhn, C., Kettner, A. J., Doyle, C. S., Brakenridge, G. R., Erickson, T. A., and Slayback, D. A.: Satellite imaging 540 reveals increased proportion of population exposed to floods, Nature, 596, 80–86, https://doi.org/10.1038/s41586-021-03695-w, 2021.

Tramblay, Y., Bouvier, C., Martin, C., Didon-Lescot, J.-F., Todorovik, D., and Domergue, J.-M.: Assessment of initial soil moisture conditions for event-based rainfall–runoff modelling, Journal of Hydrology, 387, 176–187, https://doi.org/10.1016/j.jhydrol.2010.04.006, 2010.

Tran, H., Fang, Y., Tan, Z., Zhou, T., and Leung, L. R.: Quantifying the impacts of land cover change on the hydrologic response to Hurricane Ida in the Lower Mississippi River Basin, Journal of Hydrometeorology, 10.1175/JHM-D-23-0094.1, 2024.

Tsang, M., Cheng, D., and Liu, Y.: Detecting statistical interactions from neural network weights, arXiv preprint arXiv:1705.04977, https://doi.org/10.48550/arXiv.1705.04977, 2017.

Villarini, G., Luitel, B., Vecchi, G. A., and Ghosh, J.: Multi-model ensemble forecasting of North Atlantic tropical cyclone activity, Climate dynamics, 53, 7461–7477, https://doi.org/10.1007/s00382-016-3369-z, 2019.

Wahl, T., Jain, S., Bender, J., Meyers, S. D., and Luther, M. E.: Increasing risk of compound flooding from storm surge and rainfall for major US cities, Nature Climate Change, 5, 1093–1097, https://doi.org/10.1038/nclimate2736, 2015.

Willis, T., Wright, N., and Sleigh, A.: Systematic analysis of uncertainty in 2D flood inundation models, Environmental Modelling & 550 Software, 122, 104520, https://doi.org/10.1016/j.envsoft.2019.104520, 2019.

Wing, O. E., Bates, P. D., Sampson, C. C., Smith, A. M., Johnson, K. A., and Erickson, T. A.: Validation of a 30 m resolution flood hazard model of the conterminous United States, Water Resources Research, 53, 7968–7986, https://doi.org/10.1002/2017WR020917, 2017.

Wright, S.: Correlation and causation, Journal of agricultural research, 20, 557, 1921.

Xu, D., Bisht, G., Sargsyan, K., Liao, C., and Leung, L. R.: Using a surrogate-assisted Bayesian framework to calibrate the runoff-generation scheme in the Energy Exascale Earth System Model (E3SM) v1, Geoscientific Model Development, 15, 5021–5043, https://doi.org/10.5194/gmd-15-5021-2022, 2022a.

Xu, D., Bisht, G., Zhou, T., Leung, L. R., and Pan, M.: Development of Land-River Two-Way Hydrologic Coupling for Floodplain Inundation in the Energy Exascale Earth System Model, Journal of Advances in Modeling Earth Systems, 14, e2021MS002772, https://doi.org/10.1029/2021MS002772, 2022b.

Xu, D., Bisht, G., Feng, D., Tan, Z., Li, L., Qiu, H., and Leung, L. R.: Impacts of Sea-Level Rise on Coastal Groundwater Table Simulated by an Earth System Model With a Land-Ocean Coupling Scheme, 12(8), https://doi.org/10.1029/2024EF004479, 2024.

Xu, K., Wang, C., and Bin, L.: Compound flood models in coastal areas: a review of methods and uncertainty analysis, Natural Hazards, 116, 469–496, https://doi.org/10.1007/s11069-022-05683-3, 2023.

Zarzycki, C. M., Ascher, B. D., Rhoades, A. M., and McCrary, R. R.: Algorithmically Detected Rain-on-Snow Flood Events in Different Climate Datasets: A Case Study of the Susquehanna River Basin, EGUsphere, 2024, 1–24, https://doi.org/10.5194/egusphere-2023-3094, 2024.

Zhang, W., Villarini, G., Vecchi, G. A., and Smith, J. A.: Urbanization exacerbated the rainfall and flooding caused by hurricane Harvey in Houston, Nature, 563, 384–388, https://doi.org/10.1038/s41586-018-0676-z, 2018.

Zhong, L., Li, M., and Zhang, D.-L.: How do uncertainties in hurricane model forecasts affect storm surge predictions in a semi-enclosed bay?, Estuarine, Coastal and Shelf Science, 90, 61–72, https://doi.org/10.1016/j.ecss.2010.07.001, 2010.

Zscheischler, J., Westra, S., Van Den Hurk, B. J., Seneviratne, S. I., Ward, P. J., Pitman, A., AghaKouchak, A., Bresch, D. N., Leonard, M., Wahl, T., et al.: Future climate risk from compound events, Nature climate change, 8, 469–477, https://doi.org/10.1038/s41558-018-01563, 2018.